



Universiteit
Leiden
The Netherlands

Detailed analytical characterization of a bispecific IgG1 CrossMab antibody of the knob-into-hole format applying various stress conditions revealed pronounced stability

Grunert, I.; Heinrich, K.; Ernst, J.; Hingar, M.; Briguët, A.; Leiss, M.; ... ; Bulau, P.

Citation

Grunert, I., Heinrich, K., Ernst, J., Hingar, M., Briguët, A., Leiss, M., ... Bulau, P. (2022). Detailed analytical characterization of a bispecific IgG1 CrossMab antibody of the knob-into-hole format applying various stress conditions revealed pronounced stability. *Acs Omega*, 7(4), 3671-3679. doi:10.1021/acsomega.1c06305

Version: Publisher's Version

License: [Creative Commons CC BY-NC-ND 4.0 license](#)

Downloaded from: <https://hdl.handle.net/1887/3513337>

Note: To cite this publication please use the final published version (if applicable).

Detailed Analytical Characterization of a Bispecific IgG1 CrossMab Antibody of the Knob-into-Hole Format Applying Various Stress Conditions Revealed Pronounced Stability

Ingrid Grunert,* Katrin Heinrich, Juliane Ernst, Michael Hingar, Alexandre Briguet, Michael Leiss, Manfred Wuhrer, Dietmar Reusch, and Patrick Bulau



Cite This: *ACS Omega* 2022, 7, 3671–3679



Read Online

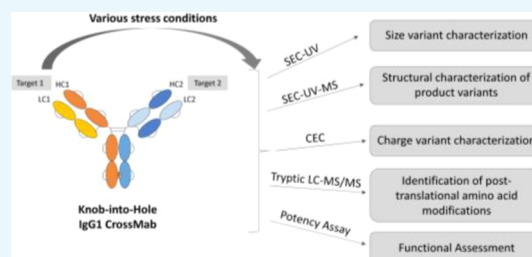
ACCESS |

Metrics & More

Article Recommendations

Supporting Information

ABSTRACT: In recent years, a variety of new antibody formats have been developed. One of these formats allows the binding of one type of antibody to two different epitopes. This can for example be achieved by introduction of the “knob-into-hole” format and a combined CrossMab approach. Due to their complexity, these bispecific antibodies are expected to result in an enhanced variety of different degradation products. Reports on the stability of these molecules are still largely lacking. To address this, a panel of stress conditions, including elevated temperature, pH, oxidizing agents, and forced glycation via glucose incubation, to identify and functionally evaluate critical quality attributes in the complementary-determining and conserved regions of a bispecific antibody was applied in this study. The exertion of various stress conditions combined with an assessment by size exclusion chromatography, ion exchange chromatography, LC–MS/MS peptide mapping, and functional evaluation by cell-based assays was adequate to identify chemical modification sites and assess the stability and integrity, as well as the functionality of a bispecific antibody. Stress conditions induced size variants and post-translational modifications, such as isomerization, deamidation, and oxidation, albeit to a modest extent. Of note, all the observed stress conditions largely maintained functionality. In summary, this study revealed the pronounced stability of IgG1 “knob-into-hole” bispecific CrossMab antibodies compared to already marketed antibody products.



INTRODUCTION

Monoclonal antibodies (mAbs) and their derivatives are the biggest and rapidly expanding class of products of the biopharmaceutical industry. The complexity of these therapeutic proteins increases with the current advance in engineering and manufacturing technologies.^{1,2} New complex product formats that deviate from the standard monoclonal IgG1 antibody structure emerge with improved specificity and efficacy, novel functionalities, and reduced undesired interactions.^{3,4} This includes among others the introduction of bispecific antibodies (bsAbs) offering new opportunities for the pharmaceutical industry. BsAbs exhibit dual target specificity to simultaneously address different epitopes on either the same or different antigens.^{4,5} Until now, four bsAbs have been approved by authorities and are available on the market (catumaxomab, blinatumomab, emicizumab, and amivantamab), two additional bsAbs were recently submitted for license application (tebentafusp, faricimab), and over a 100 are in clinical development, while others are constantly emerging.^{6,7} During the last 20 years, advances in technical antibody engineering have resulted in a range of recombinant bsAbs formats, consisting of more than 100 different formats.^{6,8} Various commercialized technology platforms exist for their creation and development.^{2,6,8,9}

Different strategies have been employed to accomplish heterodimerization of heavy chains to develop large immunoglobulin G (IgG)-like molecules. One of the techniques to enforce correct assembly is the “knob-into-hole” strategy: forcing heterodimerization by introducing specific mutations into each CH3 domain of the two heavy chains, which results in asymmetric bsAbs that can be further stabilized by implementing an artificial disulfide bridge.^{10,11} While the knob-into-hole approach enables the correct assembly of the two heavy chains, a further technique is needed to allow the correct assembly of the two light chains. One solution is the Cross-Mab technology.¹² Here, correct pairing of the light chains with the corresponding heavy chains is achieved by either exchanging the CH1 domain of one heavy chain with the constant (CL) domain of the corresponding light chain (CrossMab CH1-CL) or exchanging the light chain

Received: November 9, 2021
Accepted: December 24, 2021
Published: January 19, 2022



of one Fab arm by the Fd of the corresponding heavy chain (CrossMab Fab), or by interchanging the VH-VL interface of the Fab fragments (CrossMab VH-VL).¹³

Considerably challenging are the quantity, quality, purity, and stability of bsAbs during manufacturing and formulation, which is crucial for the safety and efficacy of these protein therapeutics.¹⁴ The complexity of these formats leads to additional modifications and changes, resulting in a larger number of undesired variants, which might differ in biophysical properties or biological function.¹⁵ Therefore, an adequate, in-depth characterization and assessment of their structural and chemical variety and consequences on the functional activity is important. Critical quality attributes (CQAs) need to be identified and monitored to ensure efficacy as well as patient safety and immunogenicity.¹⁶ Forced degradation studies are commonly applied to identify CQAs, such as post-translational modifications, and to assess the impact on the overall molecule,¹⁷ especially their effect on stability and biological function. Until now, only a few studies have addressed the impact of selected stress conditions on the stability and functionality of bsAb formats in detail.^{18–21}

Hence, the aim of this study was the thorough characterization of the chemical stability and potency of an IgG1 bispecific antibody (bsAb1) based on the CrossMab technology combined with the “knob-into-hole” format, targeting two soluble ligands (Target 1 and Target 2), after applying various stress conditions, including high temperature, low and high pH, hydrogen peroxide, and high concentration of glucose.

As introduced before, the selected bsAb1 (schematically shown in Figure 1) comprises two different heavy (HC1,

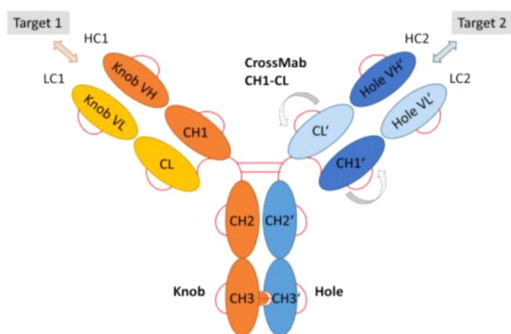


Figure 1. Schematic illustration of the bsAb1 structure, an IgG1 bispecific antibody of the knob-into-hole format combined with the CrossMab (CH1-CL) format. Red lines indicate the disulfide bonds between two cysteines.

HC2) and two different light chains (LC1, LC2), containing point mutations within the CH3 domain of the heavy chains that promote the correct assembly (“knob-into-hole”). In addition, the CH1 and CL domains in one of the target-binding Fabs were exchanged to foster the correct assembly of the two different light chains (“CrossMab”). Moreover, the neonatal Fc receptor (FcRn) and Fc gamma receptor (FcγR) binding sites of bsAb1 were modified to disable the antibody’s effector functions.^{22,23}

A comprehensive analytical platform to characterize the physico-chemical properties was applied: Structural integrity was assessed by size-exclusion chromatography (SEC) and more detailed by SEC coupled to mass spectrometry (SEC-UV-MS). Charge heterogeneity was analyzed by cation-

exchange chromatography (CEC), and the relevant chemical degradation sites were identified by tryptic LC-MS/MS peptide mapping. The effects on functionality of the generated bsAb1 variants were addressed in two independent cell-based potency assays, each measuring the ability of the bsAb to neutralize one of the two different target antigens.

RESULTS AND DISCUSSION

Preparation of Various Stress Conditions of bsAb1.

The stability, physico-chemical, and functional assessment of an IgG1 knob-into-hole bispecific CrossMab antibody (bsAb1) was examined after applying several different stress conditions. Therefore, bsAb1 reference material was exposed to elevated temperature (40 °C), low (pH 4.0) and high pH (pH 9.0), glucose (1 M glucose), and physiological (phosphate buffered saline at 37 °C) and oxidative stress (0.015% H₂O₂) as described in the Experimental Section (Table 1).

Table 1. Overview of bsAb1 Selected Stress Conditions

stress study name	applied stress condition
negative control	dialysis in formulation buffer
thermal stress	40 °C, 4 weeks
physiological stress	PBS, pH 7.4, 37 °C, 14 days
low pH stress	pH 4.0, 25 °C, 5 days
high pH + thermal stress	pH 9.0, 37 °C, 7 days
high pH stress	pH 9.0, 25 °C, 7 days
oxidative stress	0.015% H ₂ O ₂ , 25 °C, 18 h
glucose + thermal stress	1 M glucose, 37 °C, 7 days

Structural Characterization of bsAb1 Integrity by SEC-UV and Identification of Structural Variants by SEC-UV-MS. The structural integrity as well as the distribution of size variants of the stressed bsAb1 samples was assessed by size-exclusion chromatography with UV detection (SEC-UV). In addition, the size variants were identified by SEC-UV coupled to near native mass spectrometric analysis (SEC-UV-MS, see Figure 2). SEC-UV analysis revealed a low to moderate increase ($\leq 1.1\%$ difference of HMW1 or HMW2 compared to the negative control) of high-molecular-weight (HMW) forms for the low pH, thermal, and combined high pH + thermal stress bsAb1 samples. At low pH (pH 4, 25 °C, 5 days), the higher order HMW form, HMW2, was primarily formed, whereas the other applied stress conditions mostly resulted in an increase of HMW1 size variants. Furthermore, the SEC-UV data exhibited a modest increase of low-molecular-weight (LMW) forms for the thermal and high pH + thermal stress conditions compared to the negative control ($\leq 1.1\%$ difference of LMW1 or LMW2 compared to the negative control). The quantitative SEC-UV data are provided in Supporting Information Table S1. All other stress studies showed no relevant changes in size variants.

In summary, the data indicated maintained structural integrity ($\geq 95.1\%$ of main peak) of bsAb1 even following harsh stress conditions, showing relatively low amounts of fragmentation and aggregation products. To identify the detected bsAb1 size variants, near-native SEC coupled to UV and mass spectrometric detection (SEC-UV-MS) was applied. Deconvoluted intact bsAb1 spectra of the SEC-UV-MS main peak revealed four prominent peaks, each corresponding to the bsAb1 monomer containing different glycan combinations (i.e., G0F/G0F; G0F/G1F). Only the glucose stress sample at 37

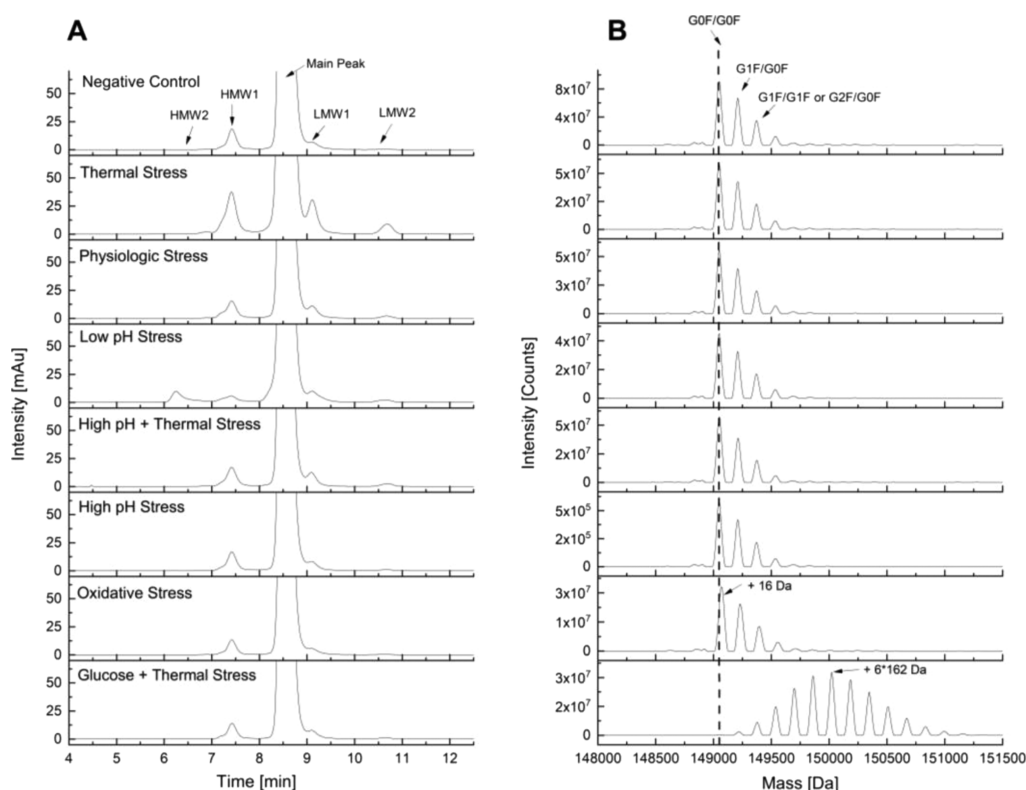


Figure 2. (A) Size variant distribution by SEC-UV and (B) deconvoluted intact mass spectra of main peak detected by near-native SEC-UV-MS of stressed bsAb1 CrossMab (for assignment of the stress conditions, see the left side of Panel A)—stacked zoom. The top chromatogram/mass spectra show exemplarily the assignment of the different variants.

°C showed a different peak pattern with multiple + 162 Da mass shifts (Figure 2).

The most intensive peak exhibited a delta mass of six times 162 Da (compared to bsAb1 monomer + G0F/G0F), which could be attributed to sixfold lysine glycation events confirmed by reduced tryptic LC-MS/MS peptide mapping (Table 3). The theoretical versus experimentally observed bsAb1 molecular mass values along with the proposed bsAb's size variant are summarized in Table 2. The findings are in accordance with earlier investigations but with lower size variant content due to implementation of an optimized purification process.²⁴

Further minor mass shifts of the deconvoluted intact mass spectra were detected for the oxidative, combined glucose + thermal, and the thermal stress sample. The observed increase in aggregates (>300 kDa, HMW2) of the low pH stress sample within SEC-UV (Figure 2) was not confirmed by SEC-UV-MS (mass detection). As those aggregates were also confirmed by sedimentation velocity analytical ultracentrifugation (data not shown), it was assumed that they are of noncovalent nature and thus not stable during electrospray ionization prior to mass detection. An in-depth characterization of fractionated bsAb1 size variants verified that these aggregates are indeed oligomeric variants (e.g., trimer; tetramer; data not shown).

The oxidative stress showed a +16 Da mass shift of the main peak. This observation can be attributed to methionine oxidation at different sites, which was confirmed by reduced tryptic peptide mapping (Table 3). In addition, SEC-UV-MS of thermal stress samples revealed a range of fragments and aggregates (increase of LMW and HMW forms) as shown in Figure 2. The aggregates can be attributed to HMW1 due to bsAb1 dimerization, whereas the LMW forms primarily

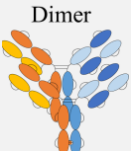


LMW1, eluting next to the monomer peak, were identified as hinge region fragmentation variants (bsAb1 without Fab, also named “des-Fab”), as described by Cordoba et al.²⁵ (Table 2, Supporting Information Figure S1). The LMW forms representing the cleaved Fab part were not detected in the initial SEC-UV-MS analysis of the nonstressed samples, probably due to their relative low abundance, but were detected using an optimized method with improved separation and MS detection conditions, revealing that the respective Fab part elutes in the LMW2 region of the SEC-UV method (data not shown). An increase of dimers (HMW2) was also observed for the combined high pH + thermal stress (pH 9, 37 °C, 7 days).

In conclusion, these results confirmed the maintained structural integrity and purity of bsAb1 size variants. Near-native SEC-UV MS revealed dimers as predominant HMW forms, as well as LMW forms resulting from hinge region fragmentation under elevated temperature conditions. This is in agreement with previous studies on antibody fragmentation events.²⁵ Moreover and most importantly, no further size variants related to the bsAb1 technology, e.g., due to chain scrambling like homodimers (pairing of two knob or two hole chains), have been detected in the bioprocessed starting material or any of the stressed bsAb1 samples.

Characterization of Charge Variants by CEC. Subsequently, the effect of the various stress conditions on the distribution of bsAb1 charge variants was assessed by CEC with UV detection. Different acidic charge variants, the main peak, and basic variants were observed (Figure 3).

A relevant increase of the acidic region was observed for almost all stress conditions (Figure 3, for the quantitative CEC evaluation, refer to Supporting Information Table S2).

Table 2. Theoretical and Observed Molecular Mass Values of bsAb1 Size Variants Detected by Near-Native SEC-UV-MS Analysis under Various Stress Conditions^a

stress study	observed molecular mass [Da]			
	HMW1	main peak (monomer)	LMW1	LMW2/ further LMW forms
Theoretical Molecular Mass [Da] and schematic illustration of size variant	298259.5 (Dimer G1F)	149048.7 (Monomer)	101163.8 (Monomer – LC2 – HC2 aa1-227, D-K) 100808.1 (Monomer – LC2 – HC2 aa1-236, C-D) 100692.9 (Monomer – LC2 – HC2 aa1-237, D-K) 100326.5 (Monomer – LC2 – HC2 aa1-240, H-T)	n.d.
				n.d.
Negative Control	298256.0	149050.7	100327.0 100798.1	n.d.
Thermal Stress	298258.7	149047.9	100326.0 100693.6 100801.0	n.d.
Physiological Stress	298256.3	149049.9	100325.5 100800.0	n.d.
Low pH Stress	298267.6	149049.3	100326.3 101169.5	n.d.
High pH + Thermal Stress	298260.2	149051.3	100325.8 100801.7	n.d.
High pH Stress	298257.0	149051.1	100326.7	n.d.
Oxidative Stress	298289.8 (=Dimer + 2*Ox)	149067.2 (=Monomer + 1*Ox)	100335.1	n.d.
Glucose + Thermal Stress	300033.2 (=Dimer + 11*162 Da)	150022.5 (=Monomer + 6*162 Da)	100813.4	n.d.

^an.d., not detected; aa, amino acid number.

For the stress conditions with elevated temperature (at 37 or 40 °C), predominantly the acidic peak 2 (AP2) increased. The basic region predominantly increased during thermal, low pH, and oxidative stress. The thermal stress condition led to a preponderant increase in basic peak 3 (BP3) and basic peak 4 (BP4), the low pH stress condition in basic peak 3 (BP3), and the oxidative stress condition in basic peak 1 (BP1).

In summary, merely the thermal and high pH stress as well as the combination of both resulted in a reduction of main peak to levels <60%, alongside with an increase of acidic charge variants (around 34–54% AP1 and AP2). Consequently, chemical and post-translational modifications were analyzed by tryptic peptide mapping to identify product variants impacting the CEC pattern. A contribution of bsAb1 fragments (predominantly due to hinge region cleavage) on the complex acidic charge variant profile can be assumed. For further

detailed identification and functional characterization of acidic bsAb1 charge variants, a comprehensive study using isolated charge will be performed in a follow-up study.

Characterization and Identification of bsAb1 Post-Translational Modifications by Reduced Tryptic LC–MS/MS Peptide Mapping. In the next step, the stressed samples were further analyzed by reduced tryptic peptide mapping combined with quantitative LC–MS/MS testing. Mildly acidic conditions were selected for proteolytic digestion to minimize artificial deamidation.²⁶ Quantitative evaluation of modified peptides and their unmodified parent peptides are summarized in Table 3. All listed peptides were identified and confirmed by MS/MS experiments.

Regarding C- and N-terminal modifications, only a minor increase of N-terminal pyroglutamic acid (pyrE) at both heavy chains under thermal (including combined thermal stresses)

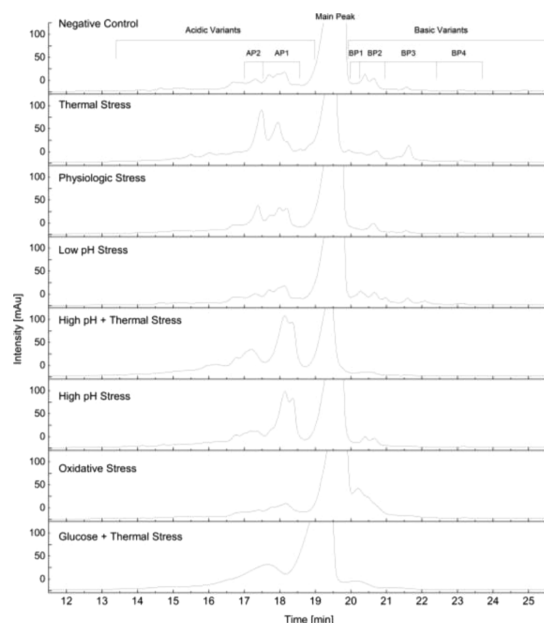


Figure 3. Characterization of bsAb1 charge variants by CEC; stacked UV chromatograms not normalized and expanded zoom. The top CEC chromatogram shows exemplarily the assignment of the different variants. AP, acidic peak; BP, basic peak.

and low pH stress was observed. The pyroglutamic acid level increased under thermal, combined high pH + thermal, and

low pH and physiological stress conditions, which is consistent with previous studies.²⁷

Across the stress panel samples, asparagine (Asn, N) deamidation/succinimide formation was shown to increase at high pH and thermal stress, in line with the increase of acidic variants observed by CEC (Figure 3).

Deamidation and isomerization induced by thermal and pH stress are common degradation pathways for therapeutic antibodies.^{27,28} The combined high pH + thermal stress sample (pH 9, 37 °C, 7 d) was most susceptible to deamidation. The most susceptible Fc Asn deamidation motif is located in the conserved IgG1 heavy chain region (CH3 domain) of therapeutic antibodies and was also found in endogenous human IgGs,^{27,29} namely, Asn390/395 (HC1) and Asn400/405 (HC2), respectively (HC1'HC2-N390/395'N400/405-deam). Of the latter, an increase of 10% within high pH + thermal stress compared to the negative control was observed. Together with the CEC data, this indicates an enrichment of Fc deamidation in the acidic AP1 peak region (Figure 3). HC1'LC2-N165'152-deam increased moderately by 2.5% within the high pH + thermal stress (pH 9, 37 °C, 7d). Only minor changes in deamidation ($\leq 1.5\%$ increase) were observed for other Asn motives, which might also be attributed to a loss of structural integrity (refer to SEC, Figure 1): LC2-N25-deam, HC2-N52/N54/N59-deam, and HC1-N84-deam. No susceptible glutamine residues were identified.

In addition, isomerization and succinimide formation at aspartic acid (Asp, D) sites were evaluated. HC2-D106 was identified to be the most susceptible site for isomerization, increasing 12.9% during thermal stress conditions followed by

Table 3. Quantitative Assessment of bsAb1 Chemical and Post-Translational Modification Sites under Various Stress Conditions by Tryptic LC–MS/MS Peptide Mapping^a

modification [%]		stress study							
	peptide name	negative control	thermal stress	physiological stress	low pH stress	high pH + thermal stress	high pH stress	oxidative stress	glucose + thermal stress
N-terminal	HC1-E1-pyrE	3.6	5.0	4.4	4.4	5.7	4.2	3.8	4.0
	HC2-Q1-pyrE	98.1	99.8	99.9	99.3	98.6	98.3	98.1	98.3
asparagine deamidation/ succinimide formation	LC2-N25-deam	0.4	0.9	0.6	0.5	1.6	0.8	0.5	0.7
	HC2-N52/N54/N59-deam	0.3	1.5	0.4	0.5	0.6	0.4	0.3	0.4
	HC1-N84-deam	0.3	0.4	0.5	0.3	1.7	0.8	0.2	0.4
	HC1'LC2-N165'152-deam	2.0	3.3	2.6	2.6	4.5	3.2	2.7	2.4
	HC1'HC2-N390/395'N400/405-deam	0.3	0.6	0.7	0.3	10.2	3.6	0.3	0.5
	HC1'HC2-N390/395'N400/405-suc	1.8	2.0	2.0	1.8	2.9	2.1	1.8	2.0
aspartate isomerization/ succinimide formation	HC2-D106-iso	3.2	16.1	7.7	3.7	6.0	3.9	1.1	6.0
	LC2-D50-iso	0.2	2.3	0.4	0.3	0.3	0.2	0.2	0.3
	LC2-D50-suc	1.6	4.3	1.5	1.5	0.9	1.4	1.4	1.1
	HC1-D405/407-iso	0.9	0.8	0.9	0.8	3.8	1.8	0.7	1.0
	HC2-D415/417-iso	0.9	0.7	0.8	0.7	3.4	1.8	0.8	0.9
methionine oxidation	HC2-M124-ox	2.2	4.1	2.9	2.8	5.4	4.9	67.3	2.8
	HC1'HC2-M258'M268-ox	1.2	1.3	1.2	1.2	1.2	1.1	22.6	1.3
	HC1'HC2-M434'M444-ox	0.7	0.8	0.7	0.7	0.7	0.6	10.0	0.8
lysine glycation	HC1-K65-gly	0.7	n.q.	n.q.	n.q.	n.q.	n.q.	n.q.	4.2
	HC1-K98-gly	2.0	n.q.	n.q.	n.q.	n.q.	n.q.	n.q.	34.5
	HC1-K252-gly	0.2	n.q.	n.q.	n.q.	n.q.	n.q.	n.q.	1.4
	LC1-K107-gly	0.2	n.q.	n.q.	n.q.	n.q.	n.q.	n.q.	1.4

^an.q., not quantified.

the isomerization at LC2-D50 (2.1%). Both Asp sites are located in the complementarity-determining regions (CDR). The increase in HC2-D106 isomerization correlates with the alterations of CEC acidic peak AP2 (Figure 3). Further characterization data of AP2 and HC2-D106 isomerization of the long-term stored drug product at 5 °C confirmed this correlation (Figure S2). The residue most susceptible to succinimide formation is LC2-D50 in the CDR (2.7% LC2-D50-suc). The increase in isomerization and succinimide formation at LC2-D50 was observed predominantly for the thermal stress correlating with an increase in the basic CEC peak BP3 (Figure 3). Within non-CDR regions, a moderate increase of 2.9% in HC1-D405/407-iso during high pH + thermal stress (pH 9, 37 °C, 7 days) and for the same motif in HC2 (HC2-D415/417) of 2.5% was observed.

HC2-M124 located in the CDR3 was identified to be the most susceptible methionine (Met, M) oxidation site increasing up to 65.1% by oxidative stress conditions followed by the conserved Fc motives Met258/268 (HC1'HC2-M258'M268-ox) showing an increase of 21.4% and Met 434/Met444 (HC1'HC2-M434'M444-ox) with 9.3% oxidation. Consequently, the oxidation of multiple methionine residues resulted in the formation of bsAb1 basic charge variants (Figure 3; BP1). No relevant oxidation ($\geq 0.5\%$) of tryptophane residues was identified by the applied stress conditions.

Finally, glycation of lysine (Lys, K) residues was assessed for the negative control and glucose stress samples. HC1-K98-gly was identified as the most susceptible glycation site (increase from 2 to 35% at the tryptic peptide level), whereas only one motif within the CDR (HC1-K65-gly) was detected to be moderately elevated following high glucose concentration.

Altogether, the application of tryptic peptide mapping indicated that the increase of the CEC basic region for the low pH stress condition was mainly attributed to the isomerization or succinimide formation of LC2-D50 (BP3) and methionine oxidation (BP1), whereas the elevation of BP4 is a consequence of aggregation at elevated temperatures as demonstrated by SEC-UV-MS. The increase in the CEC acidic region is likely to be attributed to Fc deamidation at high pH (AP1), isomerization of HC2-D106 due to thermal stress (AP2), and glycation following incubation with glucose (AP1). No chemical or post-translational modifications were found within the knob-into-hole amino acid sequence-binding region of both heavy chains.

Functional Assessment of the bsAb1 Target-Binding Potency by Cell-Based Assays. Potency was evaluated by two different bsAb1 cell-based assays to analyze the effects of the stress conditions on functionality, hence the ability to neutralize its two target ligands. The identified conserved Fc modifications, the oxidation of Met252 (according to EU numbering), which is known to impact the interaction with the FcRn receptor and thus affecting the pharmacokinetics of antibodies,³⁰ and the conserved N-glycosylation at Asn297 (EU numbering), which is known to influence effector functions,^{31,32} were not further assessed, since the FcRn and FcγR binding sites of bsAb1 were modified to disable the undesired effector functions.^{22,23}

Interestingly, only the thermal stress conditions showed a moderate impact on the target 2 neutralization (76%), as shown in Table 4. All the other forced stress conditions did not affect either target 1 or target 2 neutralization.

Table 4. Quantitative Potency Analysis of Stressed bsAb1 by Cell-Based Assays

stress study ^a	target 1 neutralization [%]	target 2 neutralization [%]
negative control	103	111
thermal stress	90	76
physiological stress	97	91
low pH stress	106	90
high pH + thermal stress	101	93
high pH stress	99	95
oxidative stress	95	93
glucose + thermal stress	94	100

^aData normalized to starting material (100%).

This demonstrates that the accelerated pH, physiological, oxidative, and glucose stress conditions did not impact the functional potency of the molecule. The decrease in target 2 neutralization (24% reduction after 4 weeks at 40 °C, Table 4) for the thermal stress indicates a correlation between the loss of bsAb1 target binding activity and the increase of HC2-D106 isomerization observed by tryptic peptide mapping, as well as with the observed fragmentation by SEC. Moreover, neither the susceptible oxidation site in the CDR3 (HC2-M124-Ox, Table 3) nor the overall glycation did negatively impact the bsAb1 functionality. Hence, none of the various stress conditions resulted in complete functional loss.

CONCLUSIONS

Forced degradation experiments followed by in-depth characterization and assessment of their structural and chemical effects, as well as the impact on the functional activity, were applied to assess the stability of a bispecific IgG1 antibody assembled by the knob-into-hole and CrossMab technology. Comparing the result from this exercise to a previous study,³³ which applied and characterized different stress conditions of a standard format IgG1 antibody, it can be concluded that the bsAb1 knob-into-hole IgG1 CrossMab technology exhibits similar degradation behavior and product stability.

In summary, the application of specific stress conditions combined with selected analytical methods for an in-depth characterization and functional evaluation were adequate for the identification and assessment of different kinds of bsAbs degradation products. For the tested bsAb1, it was demonstrated that the knob-into-hole IgG1 CrossMab technology is suitable to produce stable therapeutic antibody products, which to our knowledge has not been reported so far. Moreover, the combination of stress conditions and analytical methodologies allows the stability comparison for other biopharmaceutical technologies, such as Fc-fusion proteins³⁴ or protein scaffolds.³⁵

EXPERIMENTAL SECTION

Induction of bsAb1 Degradation Products Applying Various Stress Conditions. The recombinant bispecific IgG1 CrossMab antibody of the knob-into-hole format, bsAb1, was expressed in a Chinese hamster ovary cell system. The antibody was manufactured at Roche Diagnostics, Penzberg, Germany, using standard cell culture and purification technology. BsAb1 drug substance material was formulated at a concentration of 123 mg/mL in a His/acetate buffer system (20 mM) at pH 5.5. The below described stress studies (except

the thermal stress) were buffer exchanged by dialysis via Slide-A-Lyzer cassettes (20 K MWCO G2, 15 mL, Thermo Scientific) into formulation buffer in order to stop the stress reaction and stored frozen (at -80°C) until analysis.

Preparation of Thermal Stress Material. BsAb1 was incubated at elevated temperature (40°C) for 4 weeks and subsequently stored at -80°C until analysis.

Preparation of High pH Stress Material. BsAb1 was incubated at pH 9.0 by 1:2 dilution (sample/buffer) in 200 mM Tris-HCl (pH 9.0) followed by incubation for 7 days at different temperatures (25 and 37°C).

Preparation of Low pH Stress Material. BsAb1 was incubated at pH 4.0. Therefore, it was 1:3 diluted (sample/buffer) in 200 mM sodium acetate (pH 4.0). After dilution, the sample was incubated at 25°C for 5 days.

Preparation of Physiological Stress Material. BsAb1 was incubated under physiological conditions. Therefore, it was 1:3 diluted (sample/buffer) in $1\times$ phosphate buffered saline (PBS) and incubated for 14 days at pH 7.4 at 37°C .

Preparation of Oxidative Stress Material. BsAb1 was oxidized by adding 1% H_2O_2 stock solution to a final concentration of 0.015% H_2O_2 (v/v) for 18 h at 25°C .

Preparation of Glucose and Thermal Stress Material. BsAb1 was diluted with a glucose stock solution to a final concentration of 1 M glucose and incubated for 7 days at 37°C .

Negative Control. As a negative control (stress study control), bsAb1 was 1:3 diluted (sample/buffer) in formulation buffer followed by buffer exchange via dialysis as described for the stress study samples and stored frozen (at -80°C) until analysis.

Size Variant Analysis by SEC. SEC was carried out using a TSKgel UP-SW3000 column (4.6×300 mm, $2\ \mu\text{m}$ particle size; Tosoh Bioscience, Cat. No. 0023448). An isocratic elution using 200 mM KH_2PO_4 , 250 mM KCl, pH 6.2 at 0.3 mL/min as the solvent was used for chromatographic separation on a Dionex UltiMate3000 BioRS HPLC-system (Thermo Scientific) equipped with UV detection at 280 nm. Then, 50 μg of bsAb1 was injected for the chromatographic analysis. Data acquisition and relative quantification by manual integration and comparison of peak areas was performed by Chromeleon software (Thermo Scientific).

Charge Variant Analysis by CEC. Initial characterization of IgG charge variants was performed by CEC using a BioPro IEX-SF analytical cation exchange column (100×4.6 mm, 5 μm , Cat. No. SF00S05-1046WP, YMC) on a Dionex UltiMate3000 RSLC HPLC-system (Thermo Scientific) without carboxypeptidase B (CpB) pretreatment. Separation was achieved with a gradient from 2 to 15% eluent B in 30 min, 15 to 100% in 0.1 and 5 min at 100% eluent B (eluent A: 20 mM BES, pH 6.8; eluent B: 20 mM BES, 488 mM NaCl, pH 6.8). A flow rate of 0.8 mL/min, column temperature of 41°C , and maximum pressure of 120 bar were applied. The UV absorption was monitored at 280 nm. Approximately, 150 μg per sample was injected for chromatographic analysis. Data acquisition and relative quantification by manual integration and comparison of peak areas was performed by Chromeleon software (Thermo Scientific).

Intact Mass Spectrometry by Near-Native SEC-UV-MS. Near-native SEC-UV-MS was carried out using an ACQUITY UPLC Protein BEH SEC column (4.6×300 mm, $1.7\ \mu\text{m}$ particle size; Waters Corp.). An isocratic elution using 100 mM $\text{CH}_3\text{COONH}_4$, pH 6.0 at 0.25 mL/min, was

used for chromatographic separation with a Vanquish Horizon UHPLC system (Thermo Scientific) equipped with UV detection at 280 nm. Sample injection amounts of 12.5 μg of mAb (diluted in 0.15 M sodium phosphate pH 7.0) were used, and data acquisition was controlled by Chromeleon software (Thermo Scientific). The outlet of the UHPLC system was directly coupled to an Exactive Plus EMR mass spectrometer (Thermo Scientific). Data analysis and deconvolution was completed using Intact Mass from BYOLOGIC PMI (Protein Metrics Inc.).

Reduced Tryptic LC-MS/MS Peptide Mapping. For the detection and quantification of post-translational modifications at the peptide level, bsAb1 samples were denatured in 200 mM His/HCl, 8.0 M Gua-HCl, pH 6.0 by diluting 350 μg of bsAb1 in a total volume of 300 μL . For reduction, 10 μL of DTT solution (0.1 g/L DTT in H_2O) was added followed by incubation at 50°C for 1 h. Subsequently, a buffer exchange via an NAP-5 gel filtration column (GE Healthcare) into digestion buffer (20 mM His/HCl, pH 6.0) was performed. After buffer exchange, 10 μL of trypsin solution (0.25 mg/mL trypsin in 10 mM HCl, Trypsin Proteomics grade) was added to each NAP-5 eluate and incubated at 37°C for 18 h (based on ref 26).

Analysis of Proteolytic Tryptic Peptides by LC-MS. Approximately 4 μg of the tryptic digested samples was separated by RP-UHPLC with a C18 column (Acquity UPLC Peptide CSH C18 column, $1.7\ \mu\text{m}$, 130 Å, 2.1×150 mm, Waters) and subsequently analyzed online with an Orbitrap Fusion (Thermo Scientific) equipped with an ESI source. The mobile phases consisted of 0.1% formic acid in water (eluent A) and 0.1% formic acid in acetonitrile (eluent B). Chromatography was carried out at a flow rate of 300 $\mu\text{L}/\text{min}$ using a gradient from 1 to 12% eluent B in 31 min, 12 to 14% eluent B in 16 min, 14 to 35% eluent B in 59 min, and 35 to 80% in 2 min (lasting 3 min at 80% eluent B). Data acquisition was controlled by Orbitrap Tribrid MS Series Instrument Control Software Version 3.4 (Thermo Scientific). Parameters for MS detection were adjusted according to general experience available from peptide analysis of recombinant antibodies.

Data Analysis for the Quantification of Chemical Modifications at the Peptide Level. Peptides of interest were identified by searching manually for their m/z values within the mass spectrum and quantified with the BYOLOGIC PMI (Protein Metric Inc.) software tool. For the quantification, extracted ion chromatograms of peptides of interest were generated on the basis of their monoisotopic masses and detected charge states. The relative amounts of bsAb1 modifications were calculated from the manual integration results of the modified and unmodified peptide peaks.

Cell-Based bsAb1 Potency Assays. Both bsAb1 functionalities are considered to have independent biological effects; therefore, two independent cell-based assays addressing each of the two bsAb1 functionalities were developed. Stably transfected HEK293 cell lines with an expression vector for the respective receptor and reporter gene construct were incubated with varied bsAb1 concentrations, and the dose-dependent inhibition of the ligand-induced activities was quantified. The relative potency of a sample was calculated based on the concentration shift between reference and sample dose-response curve fits.

■ ASSOCIATED CONTENT

SI Supporting Information

The Supporting Information is available free of charge at <https://pubs.acs.org/doi/10.1021/acsomega.1c06305>.

Details on SEC-UV-MS and quantitative information of SEC-UV and CEC (PDF)

■ AUTHOR INFORMATION

Corresponding Author

Ingrid Grunert – Pharma Technical Development, Roche Diagnostics GmbH, Penzberg 82377, Germany;
orcid.org/0000-0002-5596-1015; Phone: +49/(0) 88566012918; Email: ingrid.grunert@roche.com

Authors

Katrin Heinrich – Pharma Technical Development, Roche Diagnostics GmbH, Penzberg 82377, Germany
Juliane Ernst – Pharma Technical Development, Roche Diagnostics GmbH, Penzberg 82377, Germany
Michael Hingar – Pharma Technical Development, Roche Diagnostics GmbH, Penzberg 82377, Germany
Alexandre Briguët – Pharma Technical Development, Hoffmann-La Roche, Basel 4070, Switzerland
Michael Leiss – Pharma Technical Development, Roche Diagnostics GmbH, Penzberg 82377, Germany
Manfred Wuhler – Center for Proteomics and Metabolomics, Leiden University Medical Center, Leiden 2333ZA, The Netherlands; orcid.org/0000-0002-0814-4995
Dietmar Reusch – Pharma Technical Development, Roche Diagnostics GmbH, Penzberg 82377, Germany
Patrick Bulau – Pharma Technical Development, Hoffmann-La Roche, Basel 4070, Switzerland; orcid.org/0000-0002-7121-2954

Complete contact information is available at:
<https://pubs.acs.org/doi/10.1021/acsomega.1c06305>

Author Contributions

I.G., K.H., J.E., M.H., and A.B. performed experiments and data analysis. I.G. wrote the manuscript. A.B., M.L., M.W., D.R., and P.B. reviewed the manuscript.

Notes

The authors declare no competing financial interest.

■ ACKNOWLEDGMENTS

We are indebted to all members of the laboratories at Roche in Penzberg and Basel for valuable discussions. No funding to declare.

■ REFERENCES

- (1) Spiess, C.; Zhai, Q.; Carter, P. J. Alternative molecular formats and therapeutic applications for bispecific antibodies. *Mol. Immunol.* **2015**, *67*, 95–106.
- (2) Brinkmann, U.; Kontermann, R. E. The making of bispecific antibodies. *mAbs* **2017**, *9*, 182–212.
- (3) Goulet, D. R.; Atkins, W. M. Considerations for the Design of Antibody-Based Therapeutics. *J. Pharm. Sci.* **2020**, *109*, 74–103.
- (4) Nuñez-Prado, N.; Compère, M.; Harwood, S.; Álvarez-Méndez, A.; Lykkemark, S.; Sanz, L.; Álvarez-Vallina, L. The coming of age of engineered multivalent antibodies. *Drug Discovery Today* **2015**, *20*, 588–594.
- (5) Dhimolea, E.; Reichert, J. M. World Bispecific Antibody Summit, September 27–28, 2011, Boston, MA. *mAbs* **2012**, *4*, 4–13.
- (6) Labrijn, A. F.; Janmaat, M. L.; Reichert, J. M.; Parren, P. W. H. I. Bispecific antibodies: a mechanistic review of the pipeline. *Nat. Rev. Drug Discov.* **2019**, *18*, 585–608.
- (7) Sheridan, C. Bispecific antibodies poised to deliver wave of cancer therapies. *Nat. Biotechnol.* **2021**, *39*, 251–254.
- (8) Kontermann, R. E. Dual targeting strategies with bispecific antibodies. *mAbs* **2012**, *4*, 182–197.
- (9) Kontermann, R. E. Alternative antibody formats. *Curr. Opin. Mol. Ther.* **2010**, *12*, 176–183.
- (10) Ridgway, J. B. B.; Presta, L. G.; Carter, P. 'Knobs-into-holes' engineering of antibody CH3 domains for heavy chain heterodimerization. *Protein Eng.* **1996**, *9*, 617–621.
- (11) Carter, P. Bispecific human IgG by design. *J. Immunol. Methods* **2001**, *248*, 7–15.
- (12) Surowka, M.; Schaefer, W.; Klein, C. Ten years in the making: application of CrossMab technology for the development of therapeutic bispecific antibodies and antibody fusion proteins. *mAbs* **2021**, *13*, No. 1967714.
- (13) Lewis, S. M.; Wu, X.; Pustilnik, A.; Sereno, A.; Huang, F.; Rick, H. L.; Guntas, G.; Leaver-Fay, A.; Smith, E. M.; Ho, C.; Hansen-Estruch, C.; Chamberlain, A. K.; Truhlar, S. M.; Conner, E. M.; Atwell, S.; Kuhlman, B.; Demarest, S. J. Generation of bispecific IgG antibodies by structure-based design of an orthogonal Fab interface. *Nat. Biotechnol.* **2014**, *32*, 191–198.
- (14) Chiu, M. L.; Gilliland, G. L. Engineering antibody therapeutics. *Curr. Opin. Struct. Biol.* **2016**, *38*, 163–173.
- (15) Liu, H.; Gaza-Bulseco, G.; Faldu, D.; Chumsae, C.; Sun, J. Heterogeneity of monoclonal antibodies. *J. Pharm. Sci.* **2008**, *97*, 2426–2447.
- (16) Alt, N.; Zhang, T. Y.; Motchnik, P.; Taticek, R.; Quarman, V.; Schlothauer, T.; Beck, H.; Emrich, T.; Harris, R. J. Determination of critical quality attributes for monoclonal antibodies using quality by design principles. *Biologicals* **2016**, *44*, 291–305.
- (17) Hawe, A.; Wiggenshorn, M.; van de Weert, M.; Garbe, J. H. O.; Mahler, H. C.; Jiskoot, W. Forced degradation of therapeutic proteins. *J. Pharm. Sci.* **2012**, *101*, 895–913.
- (18) Evans, A. R.; Capaldi, M. T.; Goparaju, G.; Colter, D.; Shi, F. F.; Aubert, S.; Li, L. C.; Mo, J.; Lewis, M. J.; Hu, P.; Alfonso, P.; Mehndiratta, P. Using bispecific antibodies in forced degradation studies to analyze the structure-function relationships of symmetrically and asymmetrically modified antibodies. *mAbs* **2019**, *11*, 1101–1112.
- (19) Fincke, A.; Winter, J.; Bunte, T.; Olbrich, C. Thermally induced degradation pathways of three different antibody-based drug development candidates. *Eur. J. Pharm. Sci.* **2014**, *62*, 148–160.
- (20) Baker, J. J.; McDaniel, D.; Cain, D.; Lee Tao, P.; Li, C.; Huang, Y.; Liu, H.; Zhu-Shimoni, J.; Niñonuevo, M. Rapid Identification of Disulfide Bonds and Cysteine-Related Variants in an IgG1 Knob-into-Hole Bispecific Antibody Enhanced by Machine Learning. *Anal. Chem.* **2019**, *91*, 965–976.
- (21) Manikwar, P.; Mulagapati, S. H. R.; Kasturirangan, S.; Moez, K.; Rainey, G. J.; Lobo, B. Characterization of a Novel Bispecific Antibody With Improved Conformational and Chemical Stability. *J. Pharm. Sci.* **2020**, *109*, 220–232.
- (22) Strohl, W. R. Optimization of Fc-mediated effector functions of monoclonal antibodies. *Curr. Opin. Biotechnol.* **2009**, *20*, 685–691.
- (23) Regula, J. T.; Lundh von Leithner, P.; Foxton, R.; Barathi, V. A.; Cheung, C. M.; Bo Tun, S. B.; Wey, Y. S.; Iwata, D.; Dostalek, M.; Moelleken, J.; Stubenrauch, K. G.; Nogoceke, E.; Widmer, G.; Strassburger, P.; Koss, M. J.; Klein, C.; Shima, D. T.; Hartmann, G. Targeting key angiogenic pathways with a bispecific CrossMAB optimized for neovascular eye diseases. *EMBO Mol. Med.* **2016**, *8*, 1265–1288.
- (24) Habberger, M.; Leiss, M.; Heidenreich, A. K.; Pester, O.; Hafenmair, G.; Hook, M.; Bonnington, L.; Wegele, H.; Haindl, M.; Reusch, D.; Bulau, P. Rapid characterization of biotherapeutic proteins by size-exclusion chromatography coupled to native mass spectrometry. *mAbs* **2016**, *8*, 331–339.

- (25) Cordoba, A. J.; Shyong, B. J.; Breen, D.; Harris, R. J. Non-enzymatic hinge region fragmentation of antibodies in solution. *J. Chromatogr. B Analyt. Technol. Biomed. Life Sci.* **2005**, *818*, 115–121.
- (26) Diepold, K.; Bomans, K.; Wiedmann, M.; Zimmermann, B.; Petzold, A.; Schlothauer, T.; Mueller, R.; Moritz, B.; Stracke, J. O.; Mølhøj, M.; Reusch, D.; Bulau, P. Simultaneous assessment of Asp isomerization and Asn deamidation in recombinant antibodies by LC-MS following incubation at elevated temperatures. *PLoS One* **2012**, *7*, No. e30295.
- (27) Chelius, D.; Rehder, D. S.; Bondarenko, P. V. Identification and characterization of deamidation sites in the conserved regions of human immunoglobulin gamma antibodies. *Anal. Chem.* **2005**, *77*, 6004–6011.
- (28) Lu, X.; Nobrega, R. P.; Lynaugh, H.; Jain, T.; Barlow, K.; Boland, T.; Sivasubramanian, A.; Vásquez, M.; Xu, Y. Deamidation and isomerization liability analysis of 131 clinical-stage antibodies. *mAbs* **2019**, *11*, 45–57.
- (29) Schmid, I.; Bonnington, L.; Gerl, M.; Bomans, K.; Thaller, A. L.; Wagner, K.; Schlothauer, T.; Falkenstein, R.; Zimmermann, B.; Kopitz, J.; Hasmann, M.; Bauss, F.; Habberger, M.; Reusch, D.; Bulau, P. Assessment of susceptible chemical modification sites of trastuzumab and endogenous human immunoglobulins at physiological conditions. *Commun. Biol.* **2018**, *1*, 28.
- (30) Habberger, M.; Heidenreich, A. K.; Schlothauer, T.; Hook, M.; Gassner, J.; Bomans, K.; Yegres, M.; Zwick, A.; Zimmermann, B.; Wegele, H.; Bonnington, L.; Reusch, D.; Bulau, P. Functional assessment of antibody oxidation by native mass spectrometry. *mAbs* **2015**, *7*, 891–900.
- (31) Liu, H.; Nowak, C.; Andrien, B.; Shao, M.; Ponniah, G.; Neill, A. Impact of IgG Fc-Oligosaccharides on Recombinant Monoclonal Antibody Structure, Stability, Safety, and Efficacy. *Biotechnol. Prog.* **2017**, *33*, 1173–1181.
- (32) Liu, L. M. Antibody Glycosylation and Its Impact on the Pharmacokinetics and Pharmacodynamics of Monoclonal Antibodies and Fc-Fusion Proteins. *J. Pharm. Sci.* **2015**, *104*, 1866–1884.
- (33) Habberger, M.; Bomans, K.; Diepold, K.; Hook, M.; Gassner, J.; Schlothauer, T.; Zwick, A.; Spick, C.; Kepert, J. F.; Hienz, B.; Wiedmann, M.; Beck, H.; Metzger, P.; Mølhøj, M.; Knoblich, C.; Grauschopf, U.; Reusch, D.; Bulau, P. Assessment of chemical modifications of sites in the CDRs of recombinant antibodies Susceptibility vs. functionality of critical quality attributes. *mAbs* **2014**, *6*, 327–339.
- (34) Wurch, T.; Pierré, A.; Depil, S. Novel protein scaffolds as emerging therapeutic proteins: from discovery to clinical proof-of-concept. *Trends Biotechnol.* **2012**, *30*, 575–582.
- (35) Beck, A.; Reichert, J. M. Therapeutic Fc-fusion proteins and peptides as successful alternatives to antibodies. *mAbs* **2011**, *3*, 415–416.

Recommended by ACS

Minimum Distance Between Two Epitopes in Sandwich Immunoassays for Small Molecules

Yuchen Bai, Zhanhui Wang, *et al.*

DECEMBER 15, 2022
ANALYTICAL CHEMISTRY

READ 

A Rapid Method for Direct Quantification of Antibody Binding-Site Concentration in Serum

Erwin G. Abucayon, Gary R. Matyas, *et al.*

JULY 19, 2022
ACS OMEGA

READ 

AbSE Workflow: Rapid Identification of the Coding Sequence and Linear Epitope of the Monoclonal Antibody at the Single-cell Level

Lerong Ma, Dongmei Lv, *et al.*

MAY 03, 2022
ACS SYNTHETIC BIOLOGY

READ 

Immobilization-Free Binding and Affinity Characterization of Higher Order Bispecific Antibody Complexes Using Size-Based Microfluidics

Andreas V. Madsen, Steffen Goletz, *et al.*

SEPTEMBER 27, 2022
ANALYTICAL CHEMISTRY

READ 

Get More Suggestions >